METEOR CRATER IMPACT MELT FORMATION: POTENTIAL EVIDENCE FOR CARBONATE MELTING. T. A. Gaither, J. J. Hagerty, A. Gullikson, and K. Villarreal. U.S. Geological Survey, Astrogeology Science Center, 2255 N. Gemini Drive, Flagstaff, AZ 86001, email: tgaither@usgs.gov

Introduction: Meteor Crater is a 180 m deep, 1.2 km diameter, bowl-shaped depression located in north-central Arizona [1]. This impact crater formed ~50,000 years ago [2,3] by the impact of the ~100,000 ton iron-nickel Canyon Diablo meteorite, roughly 30 m in diameter, which struck at a speed that has been estimated to be between 12 and 20 km/sec [4-7]. The crater and surrounding rim have since experienced limited erosion, providing one of the best preserved, young impact craters on Earth [8-10]. Recent sample analyses and numerical models [e.g., 12-21], indicate that the formation of Meteor Crater was much more complex than previously thought. Current numerical models are insufficient for explaining certain aspects of the impact melting process, target rock-projectile mixing, siderophile element fractionation trends, and ejecta blanket formation processes, and require further investigation to understand newly identified complexities.

These issues are being addressed through the use the USGS Meteor Crater Sample Collection, which consists of over 2,500 m of drill cuttings from 161 drill holes into the ejecta blanket of Meteor Crater. We are utilizing these drill cuttings to study the composition and spatial distribution of impact-generated materials associated with the ejecta blanket, in an effort to better understand the complexity of cratering processes and products. Here we focus on recent observations of impact melt particle (IMP) textures and compositions, carbonate inclusion (CI) compositions, and the morphologies of projectile-derived metallic inclusions (MI), and integrating these results with our detailed lithostratigraphic analysis of the ejecta deposits [22].

Methods. We have documented the textures of 36 IMPs from two drill holes in the southeastern part of the ejecta blanket (holes 94 and 95) via scanning electron microprobe (SEM), and determined the composition of a subset of these (12) via electron microprobe analysis (EMPA). All analyses were done at Northern Arizona University. Three intact, aerodynamically shaped particles, 5-10 mm in size, were selected from depth intervals throughout each drill hole. Each IMP was gently broken into several pieces to expose the particle's interior and mounted under vacuum into an individual epoxy mount. Initial SEM analysis, including energy dispersive spectroscopy (EDS) of IMPs allowed identification of areas of unaltered glass and inclusions (carbonate and metallic) for EMPA.

Results. *Impact melt textures and compositions.* Observed textures are of three types: 1) Crystalline, mostly granular pyroxene groundmass containing MI, CI, and ubiquitous fractured quartz (spherulitic and dendritic textures also observed); 2) Near pristine impact melt glass with skeletal olivine crystals, MI, and CI; and 3) Banded glass with MI and CI. The majority of the IMPs display the granular pyroxene groundmass similar to that described by [12]. Vesiculation and particulate carbonate rinds are observed on all types of IMP. Amorphous-looking carbonate rinds are also observed. Microprobe spot analyses for pristine glasses (~185) indicate variety of compositions: median values for the major elements SiO_2, CaO, MgO, and FeO are 48 wt%, 7.4 wt%, 11.6 wt%, and 30 wt%, respectively.

Carbonate inclusion textures and compositions. CIs are observed within all IMP, but show morphological differences between their host particles. Nearly all granular pyroxene groundmass samples display irregularly shaped, but sometimes spherical, carbonate inclusions, growing into the interstices between the pyroxene crystals; less common are perfectly spherical CIs within the near pristine glasses and the banded glasses. One irregularly shaped CI displays 120^{o} mineral cleavage. Microprobe analyses (341 individual spot analyses) show that the CIs are dominated by calcite compositions with trace to minor amounts of SiO_2, Al_2O_3, MnO, FeO, and NiO; MgO is present in nearly all CIs, with concentrations up to 21 wt% (median = 3.4 wt %). The bulk of the MgO concentrations fall between 1 and 14 wt%, and commonly, an individual IMP has CI compositions spanning this entire range.

Metallic inclusions textures. Most metallic inclusions are 25-100 µm in size, spherical, and, at high contrast in backscattered electron (BSE) images, display the expected compositional differences described by [16]. Irregularly shaped high-Z phases are present, often intergrown with irregular CIs in the pyroxene groundmass. Semi-quantitative energy dispersive spectrometry (EDS) analysis showed some tabular MIs have compositions consistent with barium sulfate. Submicron-size metallic inclusions were also observed at high magnification.

Lechatelierite. Vesicular, shock-melted, quartz-rich, Coconino sandstone, was observed within several IMPs.

Discussion. The observed impact melt textures and compositions are broadly similar to those described by [12] with the notable exception of the occurrence of the CIs in the groundmass. Determination of whether the CIs are target rock-derived quenched melt spherules [e.g., 14] or post-

impact aqueous alteration products [e.g., 21] is an important question to address and has implications for assessing the pressure and temperature conditions present during the formation of the crater.

We observe three types of carbonate material associated with the silicate glasses (**Fig. 1**): 1) as particulate, crystalline vesicle fillings and rinds coating the IMP exteriors, similar to [21]; 2) inclusions within pyroxene-dominated crystalline groundmass; and 3) inclusions within near-pristine and banded glasses, displaying spherical shapes with irregular fracture patterns, similar to those described in [20]. The only consistent compositional difference between these morphologies is the presence of Mg in the inclusions and lack of Mg in the vesicle fillings and rinds. The textural and compositional contrasts between the CIs and the particulate vesicle fillings and rinds suggest different formation mechanisms. Based on this compositional difference, we interpret the CIs as Kaibab-derived melt inclusions, rather than aqueous alteration products, and we interpret the textural relationship between the irregularly shaped CIs and the pyroxene groundmass as relict silicate-carbonate liquid immiscibility textures. It seems probable that the material forming the CIs was coeval with the pyroxene-forming melt and crystallized interstitially between pyroxene grains. We suggest that the occurrence of the spherical CIs in the near-pristine and banded glasses is also primary, Kaibab-derived melt, and that these melts underwent more rapid quenching that those with granular pyroxene groundmass.

Conclusions and further work. While post-impact carbonate precipitation certainly modified impact melt clasts, the evidence presented here suggests immiscible carbonate melts also participated in the formation of at least some Meteor Crater impact melts. Continuing work includes additional microprobe analyses of melt particles and their inclusions, melt source depth calculations, and analysis of submicron MI on previous interpretations of fractionation processes between projectile and target rock. These results will be combined with our ongoing lithostratigraphic analysis [e.g., 22] of the internal structure of the ejecta blanket to further explore melt formation and ejecta emplacement processes at Meteor Crater.

References: [1] Shoemaker E.M., and Kieffer S.W. (1974) *Guidebook to the geology of Meteor Crater*, Arizona, Publ. 17, 66 pp; [2] Nishiizumi K., et al. (1991) *Geochim. Cosmochim. Acta, 55*, 2699; [3] Phillips F.M., et al. (1991) *Geochim. Cosmochim. Acta, 55*, 2695; [4] Shoemaker E.M. (1960) Impact mechanics at Meteor Crater Arizona: unpublished Princeton PhD Thesis, 55 pp; [5] Melosh H.J. (1980) *Ann. Rev. Earth Planet. Sci, 8*, 65; [6] Melosh H.J. and Collins G.S. (2005) *Nature, 434*, 156;[7] Artemieva N. and Pierazzo E. (2009) *Meteor. Planet. Sci., 44*, 25; [8] Roddy D.J., et al. (1975) *Proc Sixth Lunar Sci. Conf., 3*, 2621; [9] Grant J.A., and Schultz P.H. (1993) *J. Geophys. Res., 98*, 15,033; [10] Ramsey M.S. (2002) *J. Geophys. Res., 107(E8)*, 5059;[11] Kring D.A. (2007) *LPI Contrib. No.* 1355; [12] Hörz et al. (2002) *Meteor. Planet. Sci., 37*, 501; [13] Mittlefehldt et al. (2005), *GSA Special Paper, 384*, 367; [14] Osinski et al. (2008) *Meteor. Planet. Sci., 43*, 1939; [15] Artemieva N. and Pierazzo E. (2011) *Meteor. Planet. Sci., 46*, 805; [16] Gaither et al., (2012) *LPSC 43*, abstract #1601; [17] Hagerty et al. (2012) *75th Ann. Meeting Meteor. Soc.*, abstract #5296; [18] Hagerty et al., (2010) *LPSC 41*, abstract #2213; [19] Hagerty et al., (2011) *PCC* 2, abstract #1109; [20] Osinski et al. (2008) *GSA Special Paper, 437*, 1; [21] Hörz et al. (2015) *Meteor. Planet. Sci., 50*, 6. [22] Gullikson et al. (2015) PCC 6, this volume.

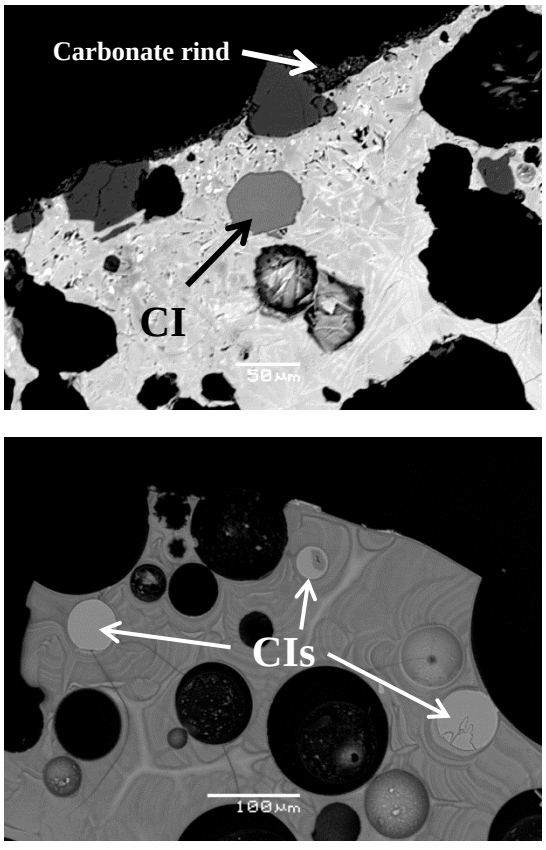

Figure 1. *Top*: SEM BSE image of CI within granular pyroxene groundmass; particulate carbonate rind at top center. *Bottom*: CIs in banded glass. Difference in CI shading between images is due to higher BSE contrast in top image.